Supporting Information

Revealing Axial-Ligand-Induced Switching of Spin States for Controllable Single Electron Transfer-based Radical Initiation

Jingyi Qin,[a] Yiyan Yin,[a] Xiaowen Guan,[a] Xiyang Ge,[a] Mengyu Cao,[a] Jin Ouyang,[b] Na Na*[a]

Table of Contents

Experimental details

Chemicals

4-nitrobenzenethiol, 2,4-dimethylbenzenethiol, Nitrotetrazolium blue chloride (NBT), 1-methoxy-4-vinylbenzene, 4-methoxythiophenol, 4-chlorothiophenol, Styrene, Ammonia solution (25%-30%), Tetrakis (4-carboxyphenyl) porphyrin (TCPP), 2,2,6,6-tetramethylpiperidinooxy (TEMPO), Deuterium oxide (99.9 atom% D) were purchased from Beijing InnoChem Science & Technology Co., Ltd. Fe(III)meso-tetra(4-carboxyphenyl)porphine chloride (Fe(III)Cl-TCPP), trimethyl(phenyl)silane and 4-(trifluoromethyl)thiophenol were obtained from Shanghai Aladdin Biochemical Technology Co., Ltd. All chemicals were used without any further purification. Deionized water (Milli-Q, Millipore, 18.2 MΩ) was used in this work.

Electron paramagnetic resonance (EPR) spectroscopy

Electron paramagnetic resonance (EPR) spectra were obtained by a Bruker-A300 spectrometer (German). DMPO was used as the trapping agent to capture the thiyl radical or $O_2^{\bullet-}$. Fe(III)Cl-TCPP was added into substrate **1a**, and 30 s later, DMPO was added for testing (to obtain Figure 1d). The above reaction was treated in N_2 atmosphere to obtain the blue EPR spectrum in Figure 2a. Similarly, with TCPP and DMPO added into substrate **1a**, the yellow EPR data in Figure 2a were recorded under air conditions. To reveal the spin states of intermediates, low-temperature EPR analysis was carried out at 77 K (in a liquid nitrogen cooled finger dewar). In the experiment, Fe(III)Cl-TCPP was added into 10 mM substrate **1a** (DCM as solvent), which was immediately transferred to the EPR tube for the detection. Besides, the above reaction was subjected to nitrogen conditions to collect the corresponding data in Figure S7.

Raman spectroscopy

Raman spectra were collected using Horiba HR Evolution (Sunano, China) with a 488 nm laser as the excitation source. The preparation of samples was the same as the EPR experiments. All data were collected at 77 K (in a liquid nitrogen cooled finger dewar).

Other instruments

UV–vis absorbed spectra were measured by a UV 2600 spectrophotometer (Shimadzu, Japan). The X-ray photoelectron spectra (XPS) were recorded using a Thermo Scientific Nexsa (USA) equipped with an Al Kα excitation source. GC-MS data were collected on Agilent 7890 GC System with an Agilent 5975 Mass Selective Detector (USA). ^{1}H NMR and ^{13}C NMR spectra were recorded on JEOL-600 spectrometers (Japan).

Mass spectroscopy

On-line monitoring was performed on an LTQ XL (Thermo Fisher Scientific, USA) instrument using a homemade ionization source of Venturi easy ambient sonic-spray ionization mass spectrometry (V-EASI-MS). The reaction solution was extracted from a capillary (inner diameter of 200 μm) and ionized by a high-velocity (sonic) nebulizing stream of N_2 gas through an external capillary. The operational parameters were as follows: full-scan positive (+) ion spectra were obtained over the m/z range from 100 to 1300; the temperature of the MS inlet capillary was 275°C. The maximum ion injection time was 1000 ms. All MS results were obtained and processed using the Xcalibur or Microcal Origin (version 8.0) software.

Treatment of catalyst Fe(III)Cl-TCPP

In order to capture the catalyst signal by V-EASI-MS, Fe(III)Cl-TCPP was treated with ammonia solution, and the substituent benzoic acid groups around the porphyrin were changed to ammonium benzoate. This treatment increased the water solubility of catalysts, which facilitated the monitoring of the whole reaction system by mass spectrometry. Based on the UV and XPS data, the Fe^{III} was confirmed to be coordinated with N atoms at the porphyrin center after treatments (Figure S1). 0.1 mmol of Fe(III)Cl-TCPP and 1 mL of ammonia solution were mixed in 50 mL water and stirred until it was completely dissolved to be a dark green solution. Upon rotary evaporation, the solvent was removed to obtain dark green solid of Fe(III)Cl-TCPP-NH_4^+. Given the remaining of basic structure, Fe(III)Cl-TCPP-NH_4^+ was abbreviated into Fe(III)Cl-TCPP.

General procedure for radical thiol-ene reactions

For radical thiol-ene reactions, 0.25 mmol of olefin was added into the mixture of 0.25 mmol thiol, 0.55 mg Fe(III)Cl-TCPP (0.25 mol%) and CH_3CN (0.5 mL), and stirred at room temperature for 5-10 min in air. Some reactions described herein are executed under special conditions. The reaction procedure carried out in nitrogen is the same as above, except that nitrogen gas is continuously introduced during the reaction process. The reaction procedure carried out using TCPP (0.25 mol%) as the catalyst is the same as that in air except that the catalyst is replaced with TCPP. Subsequently, the mixture was purified by silica gel column chromatography (petroleum ether/ dichloromethane = 50:1, v/v) to afford the corresponding product **3**.

Preparation of deuterium substituted substrate 1a

Deuterium oxide (2 mL) and 2,4-dimethylbenzenethiol (500 μL) were mixed and sonicated for 5 min. After minutes of standing until stratification, the deuterated product was obtained by extracting the upper organic solvent.

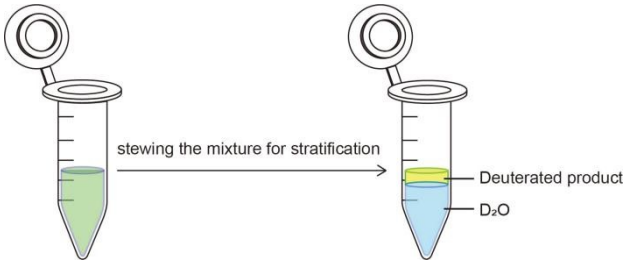

Computational procedure

Quantum chemical calculations were performed using density functional theory (DFT) at the BP86/Def2-TZVP level with the Gaussian 09 program package.[1] All calculations were carried out using unsubstituted porphyrin and thiophenol as models. Vibrational frequencies were calculated at the same level to confirm the minimum structure (no imaginary frequency). The adsorption energy was calculated based on the difference between A-B total energy and the energy sum of isolated A and B, $E_{ads} = E_{A-B} - E_A - E_B$. The electrostatic potential analysis was evaluated by Multiwfn program,[2-3] and all isosurface maps were rendered by the VMD program[4]. Since Fe(III)-porphyrin is a positive ion, the entire molecule should have a more positive potential relative to substrate and oxygen. In order to distinguish the potential of IN1 more clearly, Fe(III)-porphyrin and its axial ligands were individually displayed by the molecular electrostatic potential distribution.

Characterization of reaction products

(2,4-dimethylphenyl)(phenethyl)sulfane (3a)

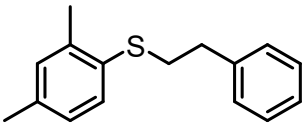

Colorless oil; 111.5 mg, 92% isolated yield.

^{1}H NMR (600 MHz, Chloroform-*d*) δ 7.39 – 7.27 (m, 6H), 7.10 (s, 1H), 7.07 (d, J = 8.0 Hz, 1H), 3.23 – 3.15 (m, 2H), 3.04 – 2.97 (m, 2H), 2.46 (s, 3H), 2.38 (s, 3H).

^{13}C NMR (151 MHz, Chloroform-*d*) δ 140.41, 138.19, 135.93, 131.75, 131.11, 129.29, 128.46, 127.14, 126.36, 35.62, 34.98, 20.86, 20.40.

(4-methoxyphenyl)(phenethyl)sulfane (3b)

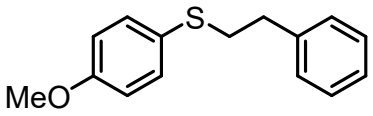

^{1}H NMR (600 MHz, Chloroform-*d*) δ 7.41 – 7.31 (m, 2H), 7.33 – 7.11 (m, 5H), 6.88 – 6.82 (m, 2H), 3.80 (s, 3H), 3.06 (d, J = 4.6 Hz, 2H), 2.87 (s, 2H).
^{13}C NMR (151 MHz, Chloroform-*d*) δ 159.04, 140.47, 133.36, 128.60, 128.55, 126.43, 114.70, 55.44, 37.33, 36.00.

(4-chlorophenyl)(phenethyl)sulfane (3c)

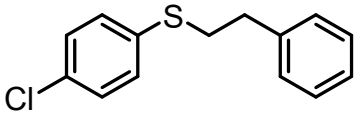

^{1}H NMR (600 MHz, Chloroform-d) δ 7.30 (dd, J = 10.5, 4.4 Hz, 2H), 7.27 – 7.21 (m, 5H), 7.19 (dd, J = 7.9, 0.9 Hz, 2H), 3.17 – 3.12 (m, 2H), 2.91 (dd, J = 8.7, 7.0 Hz, 2H).
^{13}C NMR (151 MHz, Chloroform-*d*) δ139.90, 134.89, 131.95, 130.56, 129.02, 128.53, 128.47, 126.53, 35.50, 35.37.

Phenethyl(4-(trifluoromethyl)phenyl)sulfane (3d)

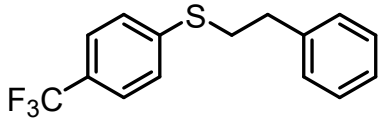

^{1}H NMR (600 MHz, Chloroform-d) δ 7.54 – 7.50 (m, 2H), 7.37 (d, J = 8.2 Hz, 2H), 7.34 – 7.30 (m, 2H), 7.26 – 7.20 (m, 3H), 3.25 – 3.21 (m, 2H), 2.99 – 2.95 (m, 2H).
^{13}C NMR (151 MHz, Chloroform-*d*) δ 142.09, 142.08, 139.67, 128.61, 128.48, 127.45, 126.68, 125.66 (q, J = 3.7 Hz), 35.23, 33.94.

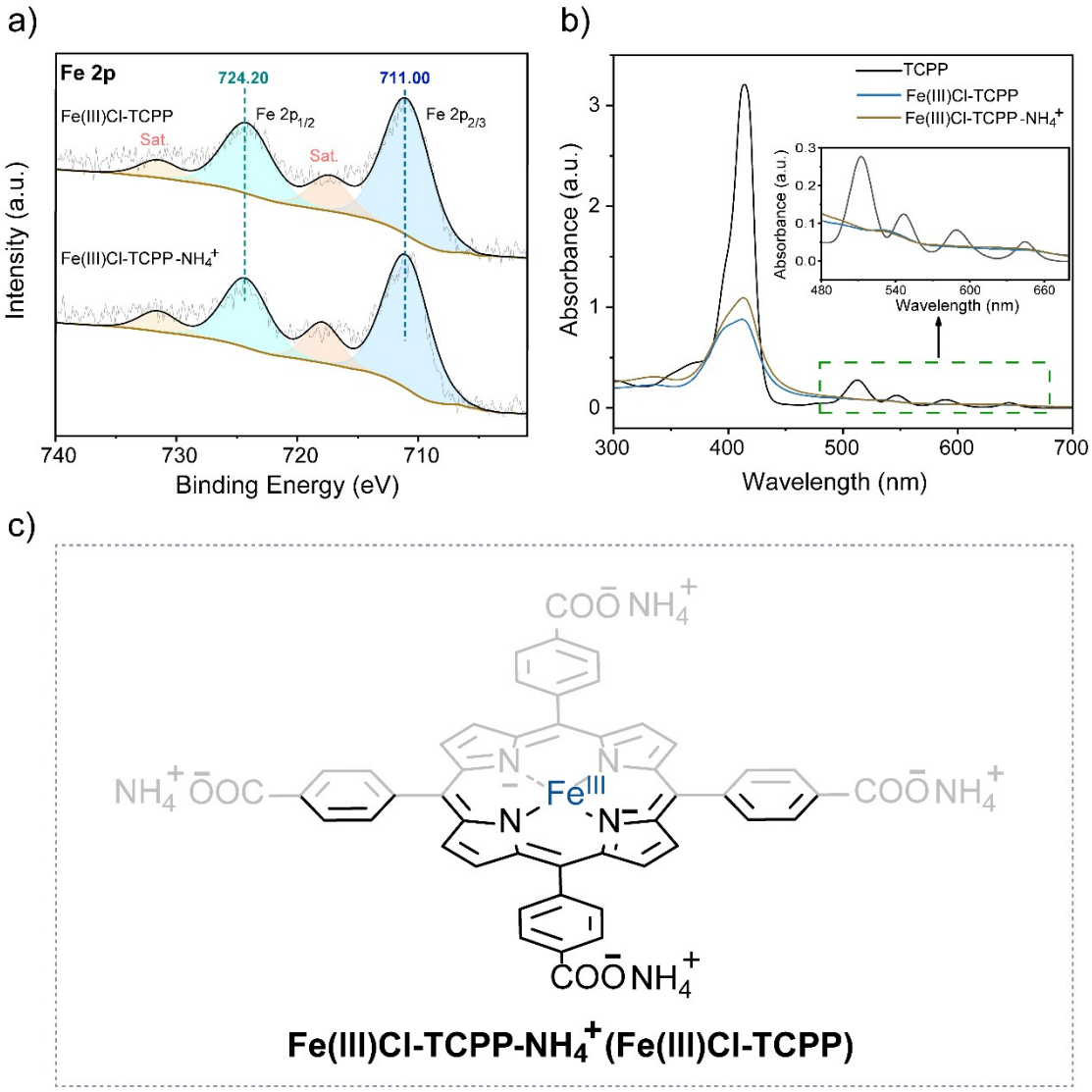

Figure S1. Characterizations of catalyst after ammonia treatments. (a) Fe 2p XPS spectra of Fe(III)Cl-TCPP and Fe(III)Cl-TCPP-NH_4^+. (b) UV-vis absorption of TCPP, Fe(III)Cl-TCPP and Fe(III)Cl-TCPP-NH_4^+. (c) The chemical structure of Fe(III)Cl-TCPP-NH_4^+ (Fe(III)Cl-TCPP).

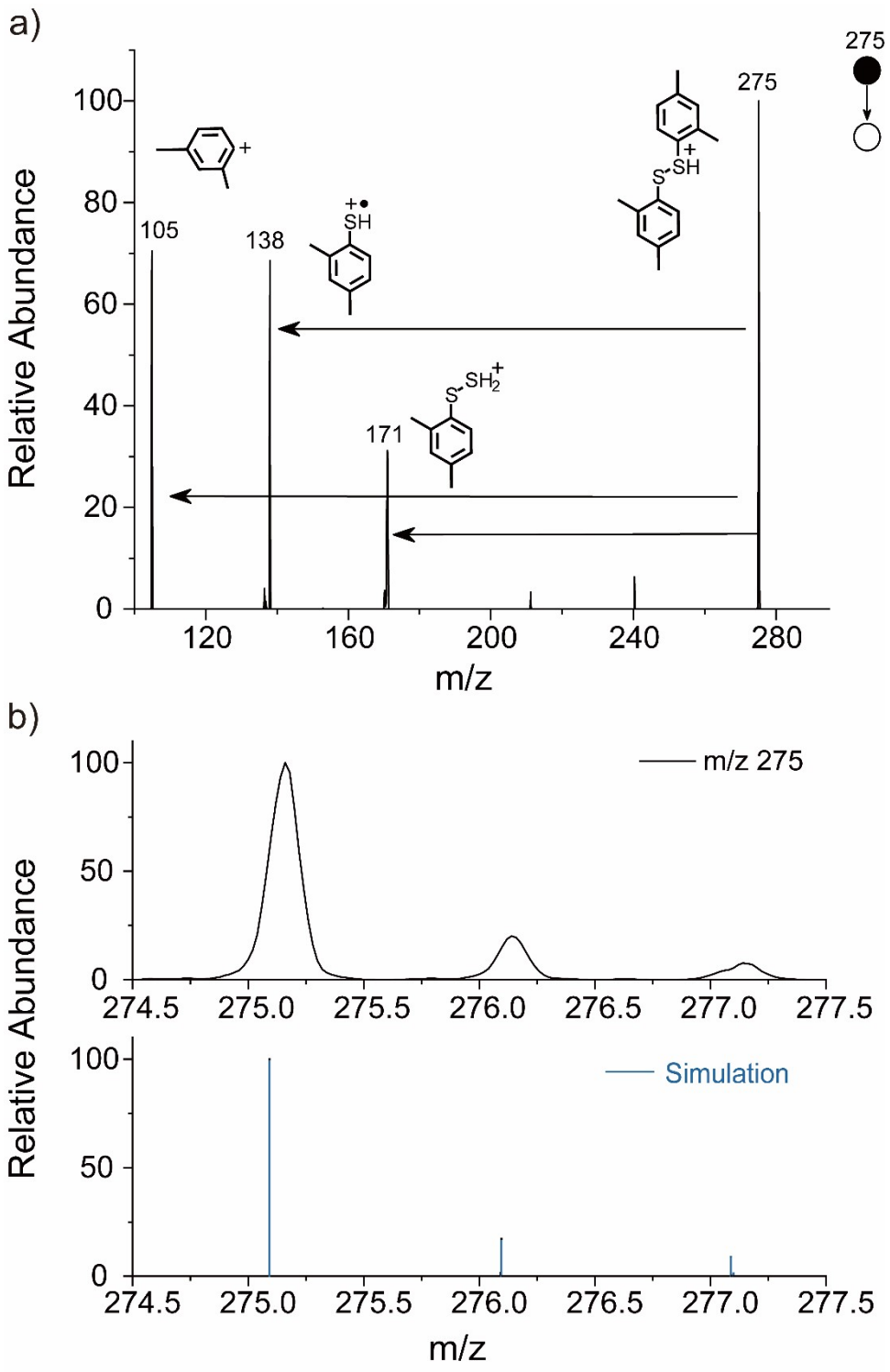

Figure S2. CID diagrams (a) and HR-MS (b) of the ion at m/z 275.

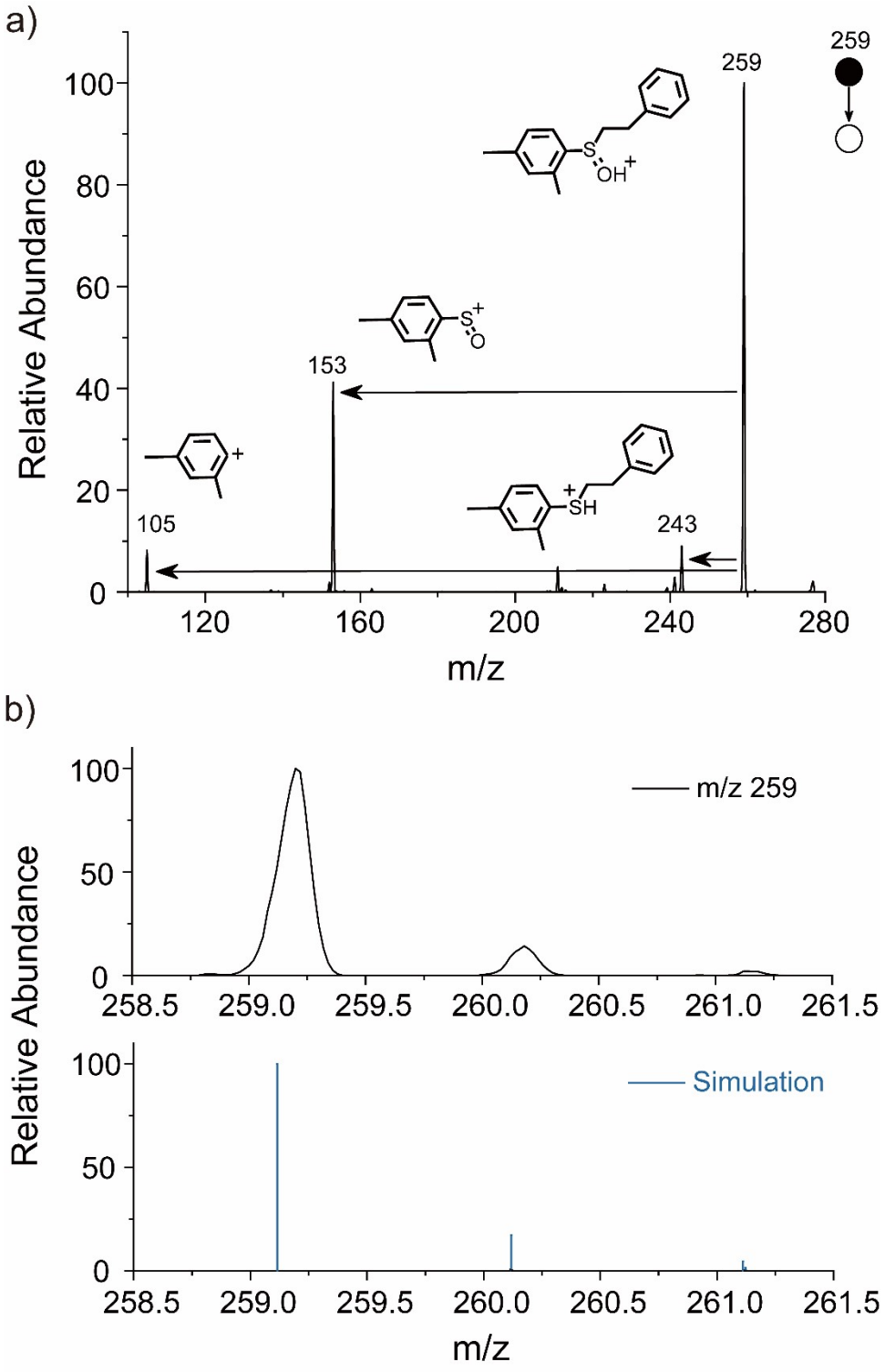

Figure S3. CID diagrams (a) and HR-MS (b) of the ion at m/z 259.

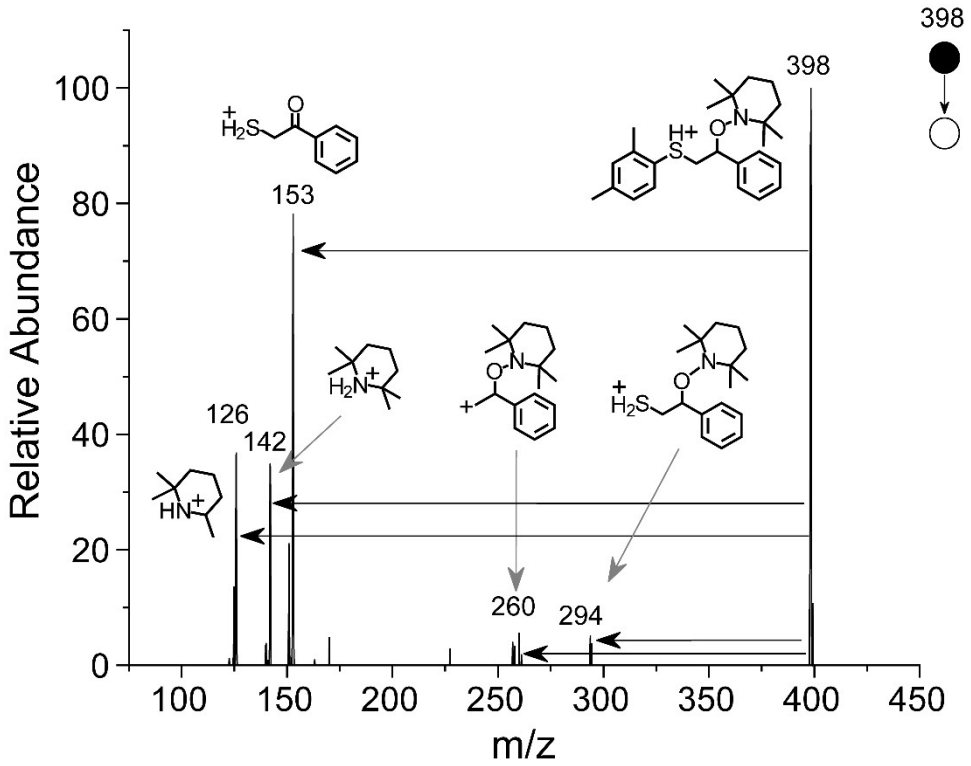

Figure S4. CID diagrams of the ion at m/z 398.

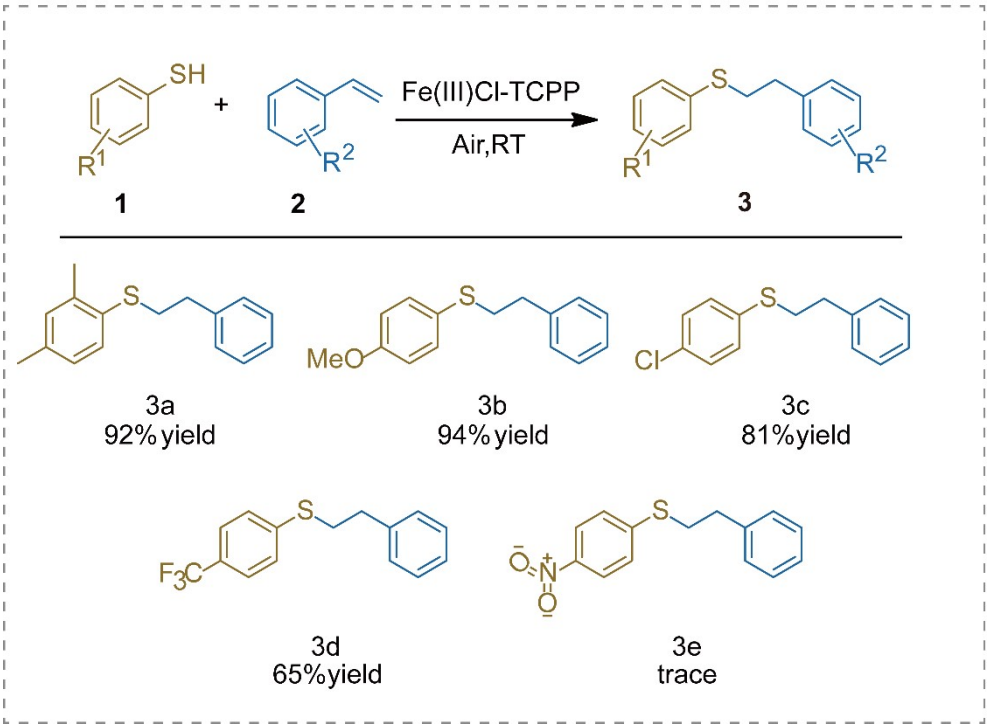

Figure S5. Catalytic performance of Fe(III)Cl-TCPP as catalyst for TEC reaction. Conditions: **1** (0.5 mmol), **2** (0.5 mmol), and Fe(III)Cl-TCPP (0.25 mol%). Yields were determined by GC-MS analysis with trimethyl(phenyl)silane as an internal standard.

Figure S6. Yield of model reaction in different reaction solvents. Conditions: **1a** (0.25 mmol), **2a** (0.25 mmol) and Fe(III)Cl-TCPP in 0.5 mL solvent, 25°C for 5 min.

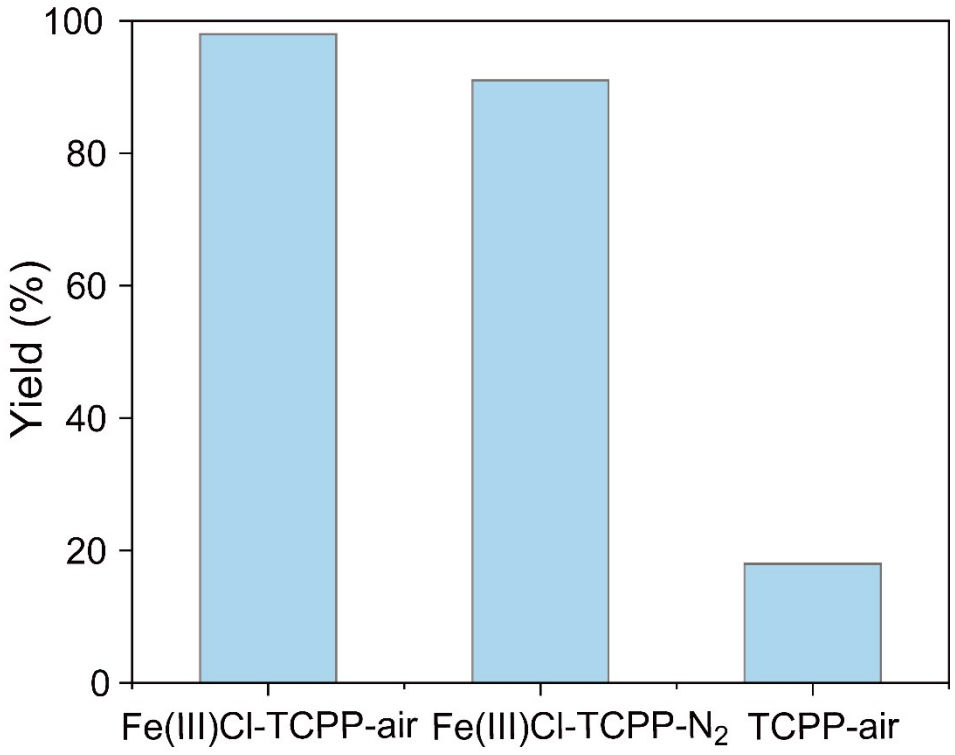

Figure S7. The comparison of TEC yields under different conditions.

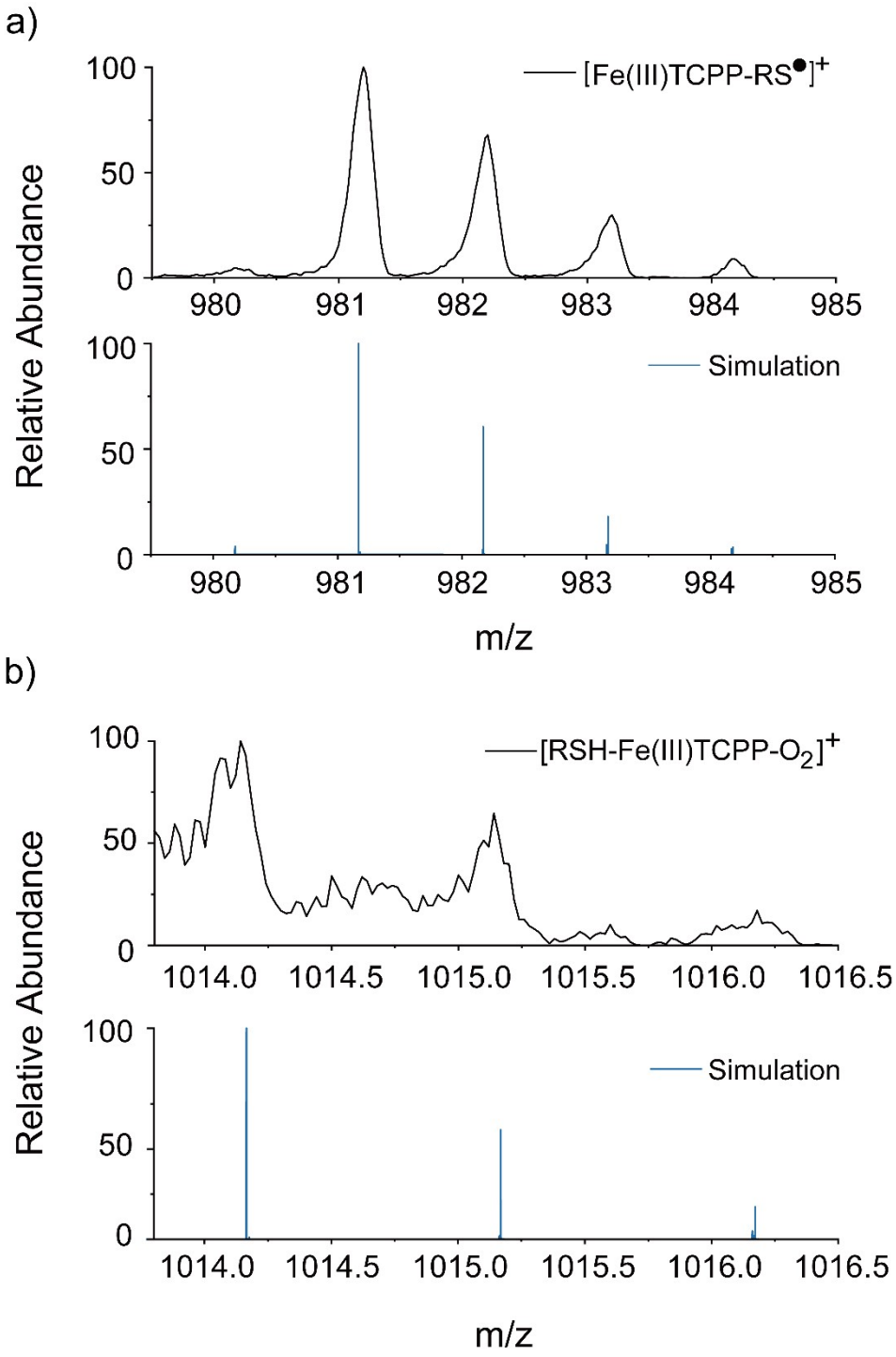

Figure S8. HR-MS of ions at m/z 981 (a) and 1014 (b).

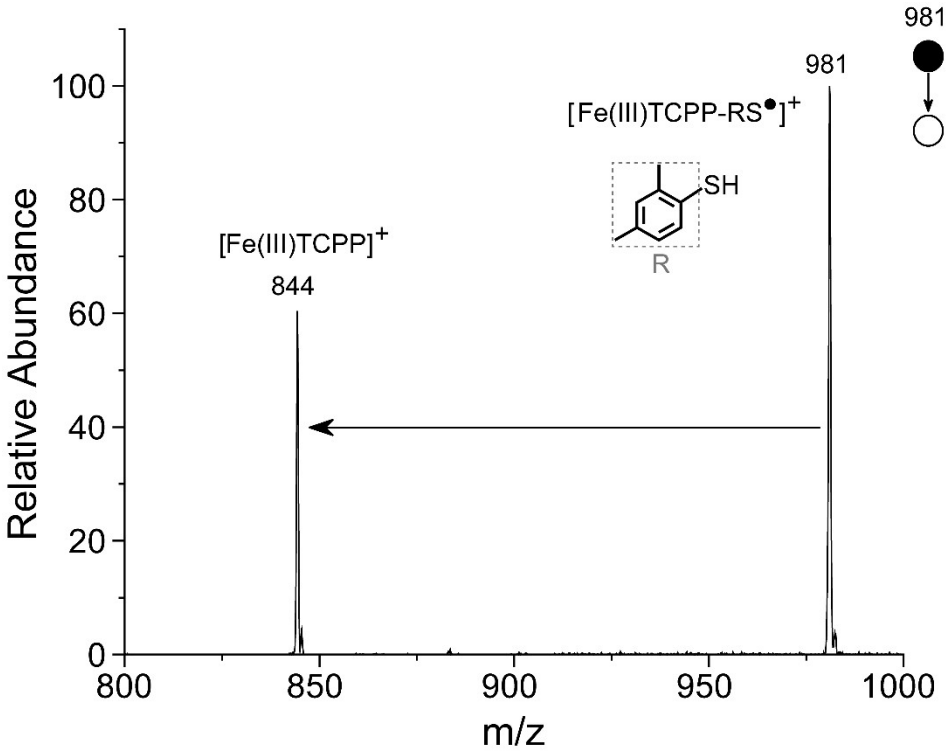

Figure S9. CID diagrams of the ion at m/z 981.

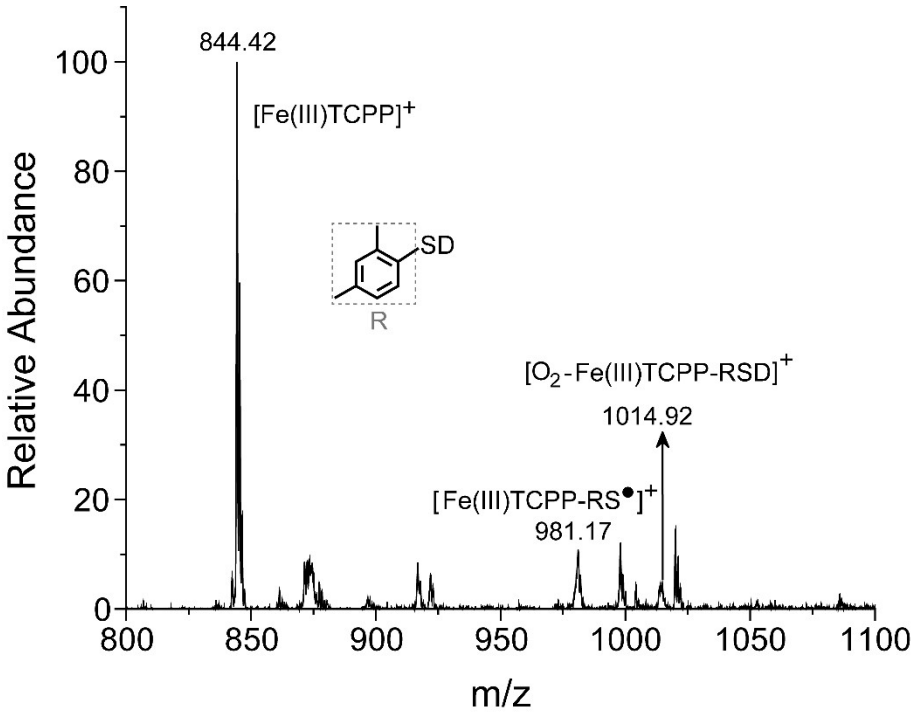

Figure S10. Mass spectra of the mixture of deuterium substituted substrate **1a** and Fe(III)Cl-TCPP.

Figure S11. CID diagrams of the ion at m/z 1086.

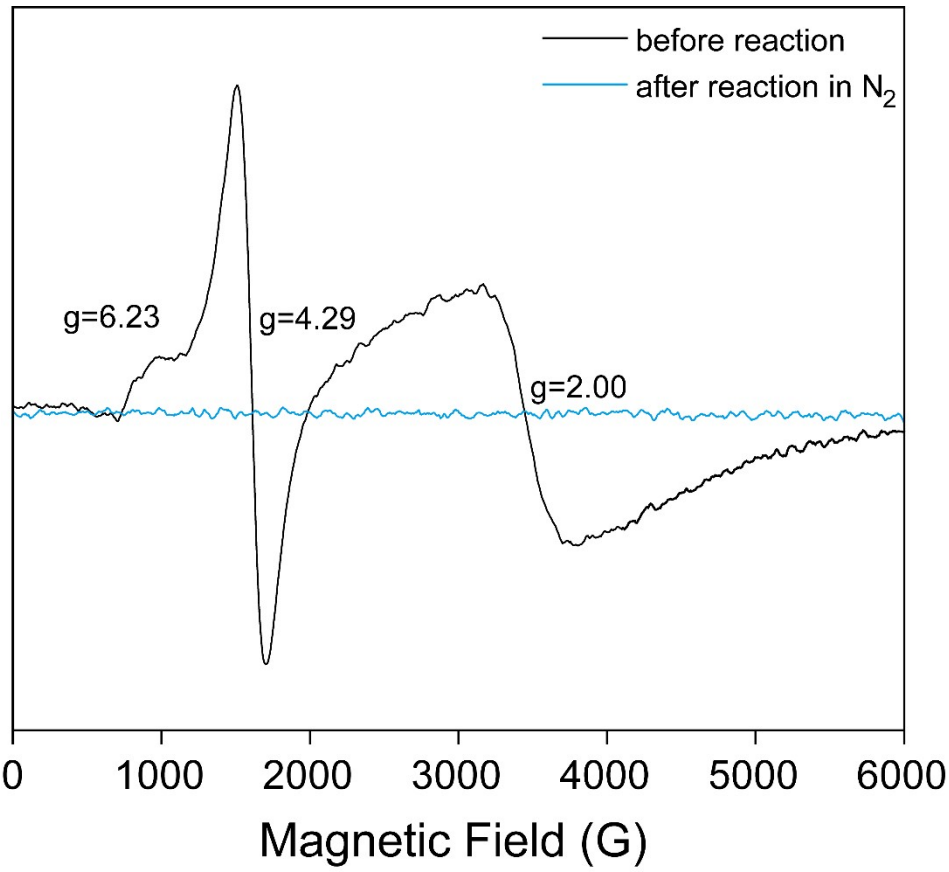

Figure S12. EPR spectra of catalyst Fe(III)Cl-TCPP before and after the reaction in N_2.

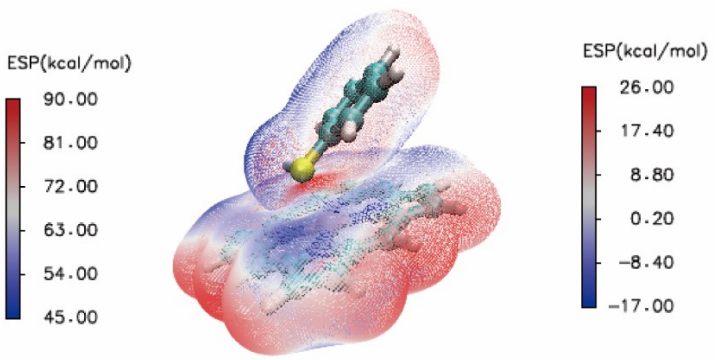

Figure S13. Molecular electrostatic potential of IN1. The left axis corresponds to the iron porphyrin and the right axis corresponds to the axial ligands.

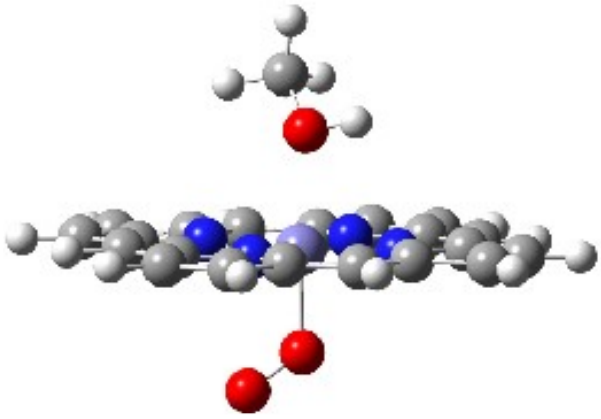

Figure S14. DFT - optimized structure of complex with CH_3OH bound.

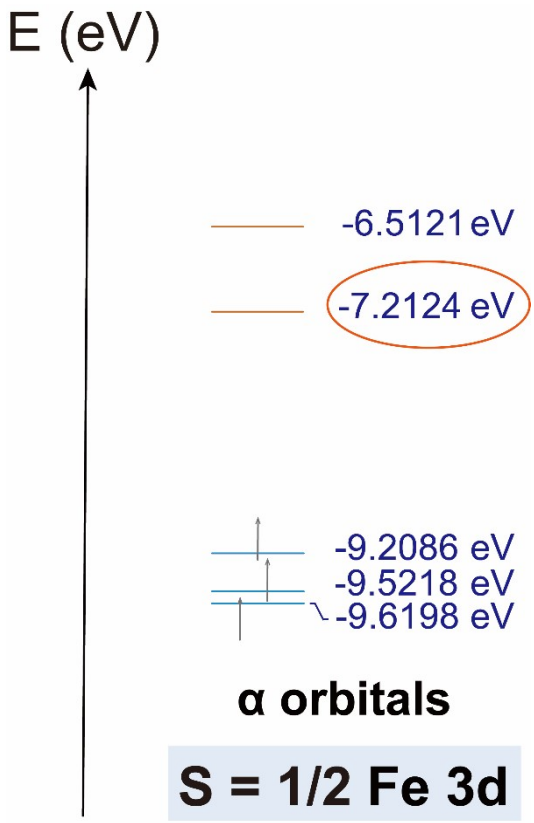

Figure S15. Calculated molecular orbitals of S = 1/2. The blue lines represent the occupied 3d orbitals, and the orange lines represent the unoccupied 3d orbitals.

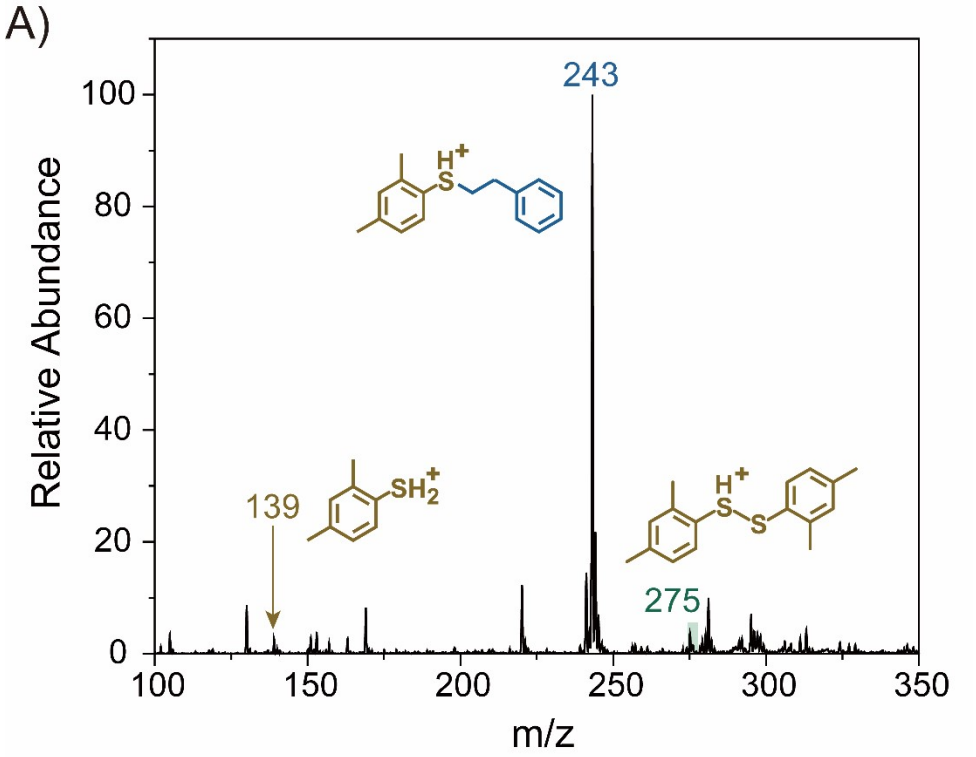

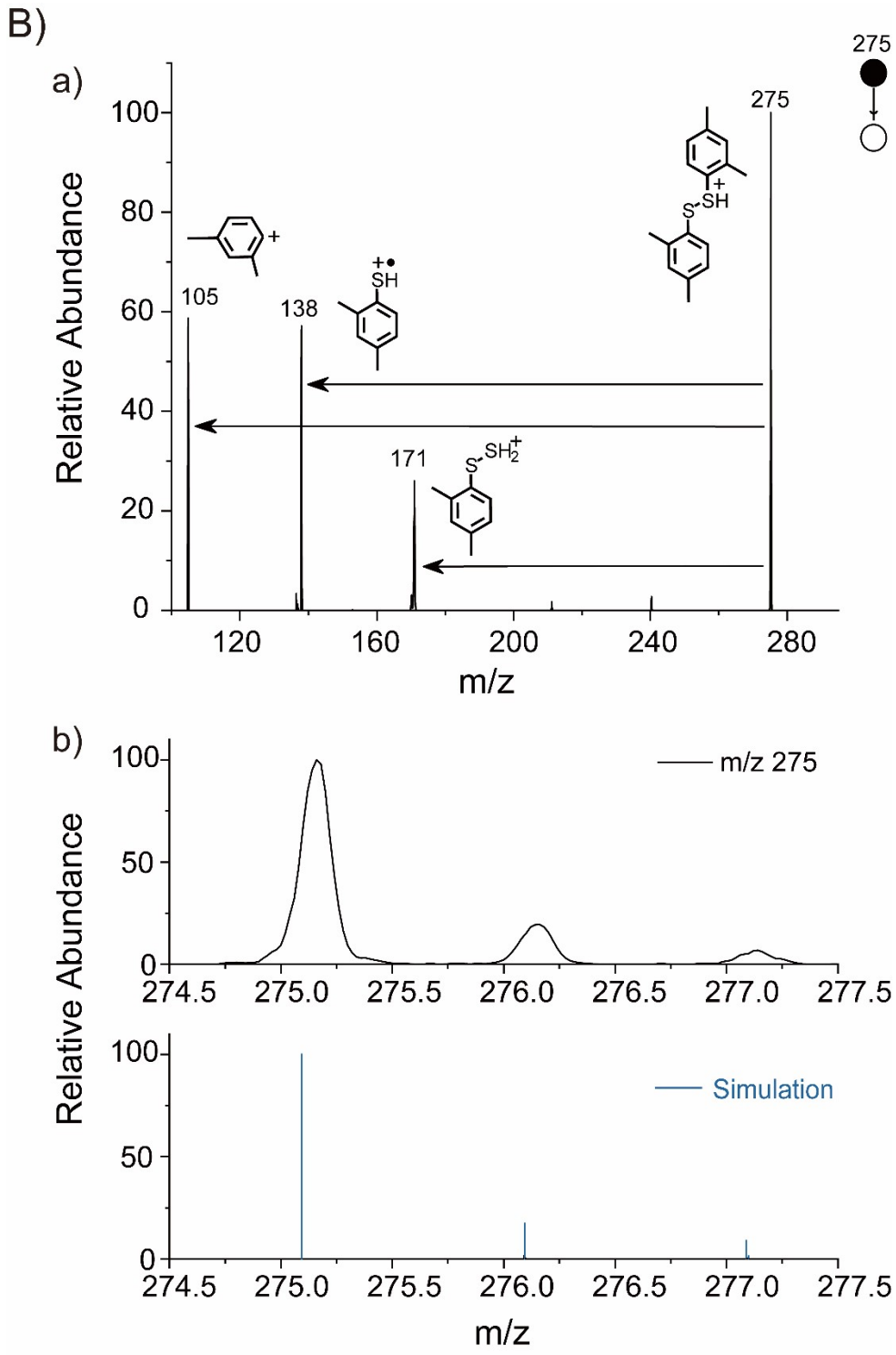

Figure S16. Evaluation on the possibility for homo-coupling reactions to generate disulfide product. (A) Mass spectrum of the reaction system for 5 min in N_2. Reaction conditions: **1a** (0.5 mmol), **2a** (0.5 mmol) and Fe(III)Cl-TCPP(0.25 mol%) in 3 mL solvent (CH_3CN:H_2O=10:1, v:v). (B) CID diagrams (a) and HR-MS (b) of the ion at m/z 275.

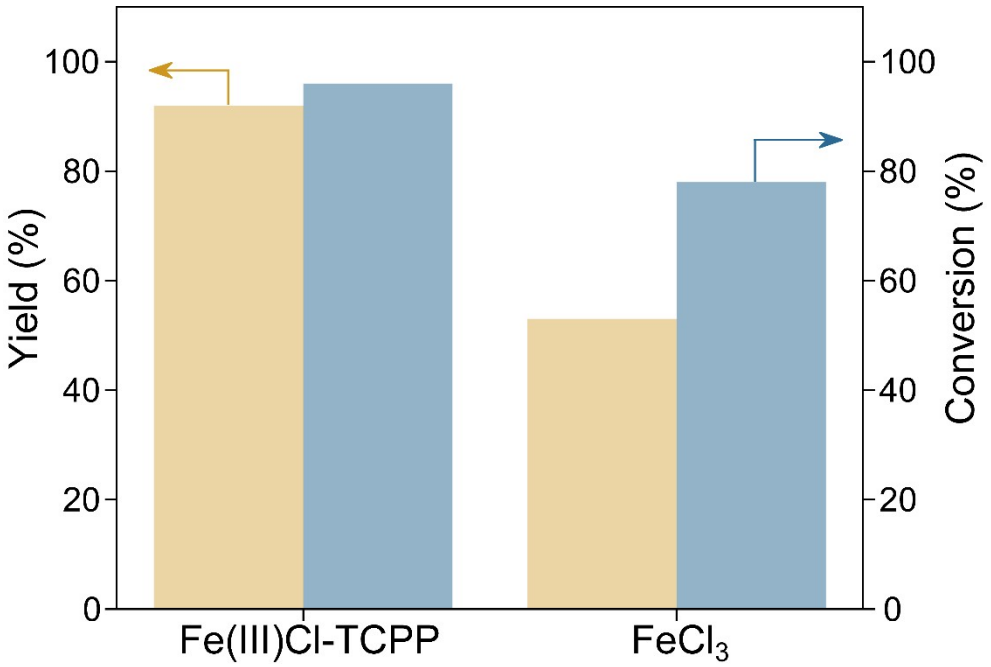

Figure S17. Comparison of the reaction performance with free Fe^{III} and Fe(III)Cl-TCPP as the catalysts.

1.

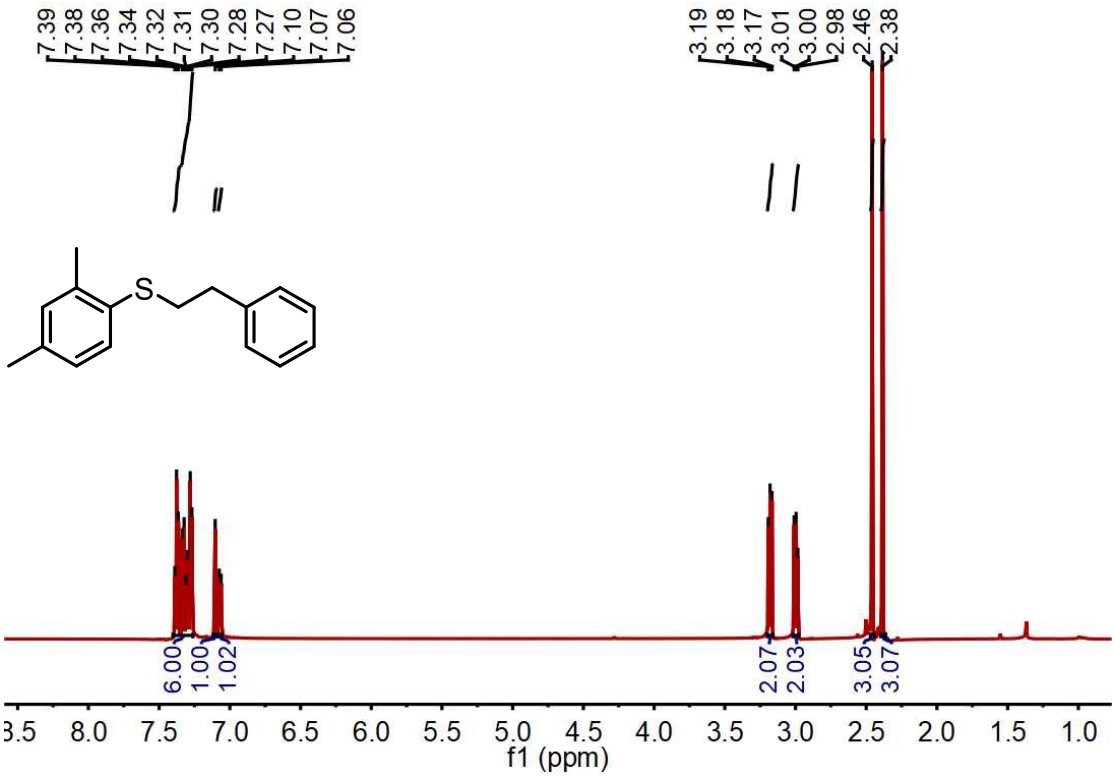
7.39
7.38
7.36
7.34
7.32
7.31
7.30
7.28
7.27
7.10
7.07
7.06
3.19
3.18
3.17
3.01
3.00
2.98
2.46
2.38
S
6.00
1.00
1.02
2.07
2.03
3.05
3.07
f1 (ppm)

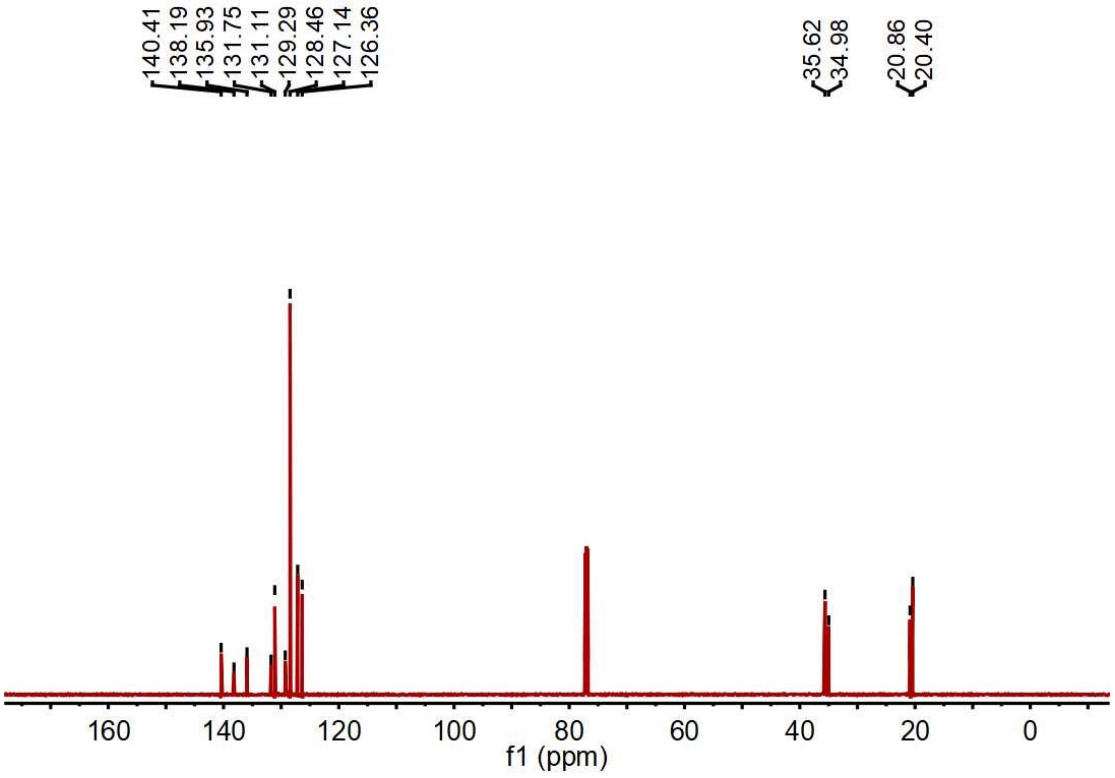
140.41
138.19
135.93
131.75
131.11
129.29
128.46
127.14
126.36
35.62
34.98
20.86
20.40
f1 (ppm)

2.

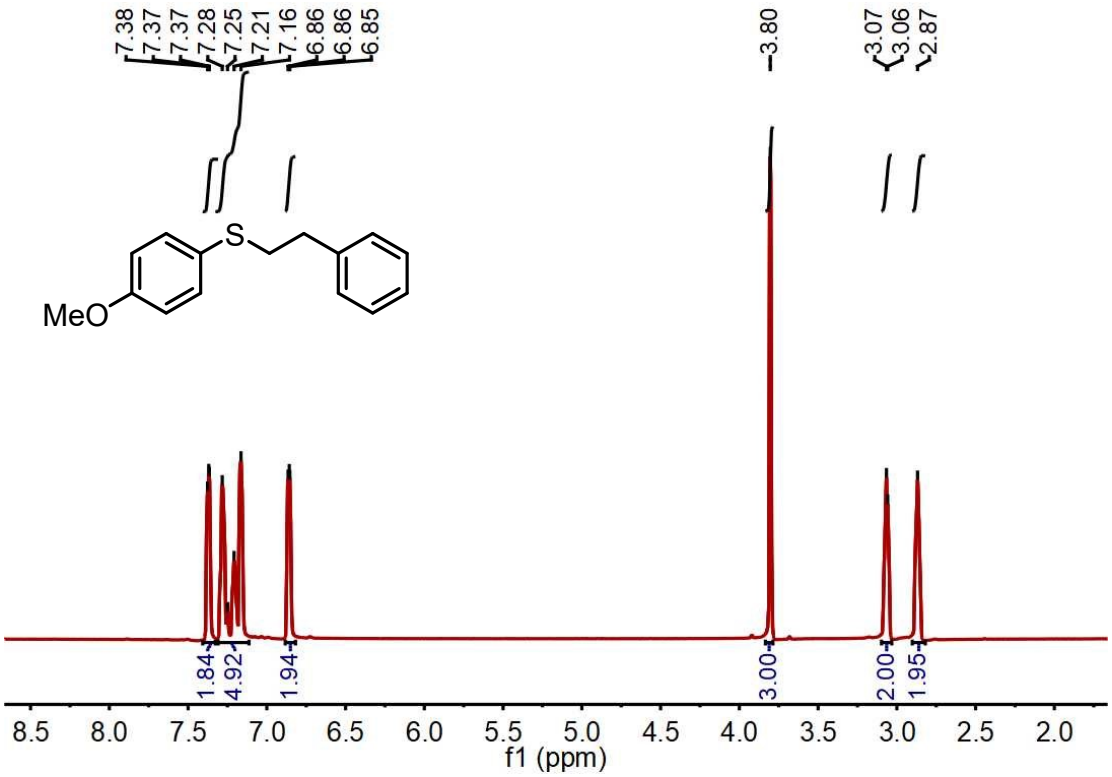
7.38
7.37
7.37
7.28
7.25
7.21
7.16
6.86
6.86
6.85
3.80
3.07
3.06
2.87
S
MeO
1.84
4.92
1.94
3.00
2.00
1.95
8.5
8.0
7.5
7.0
6.5
6.0
5.5
5.0
4.5
4.0
3.5
3.0
2.5
2.0
f1 (ppm)

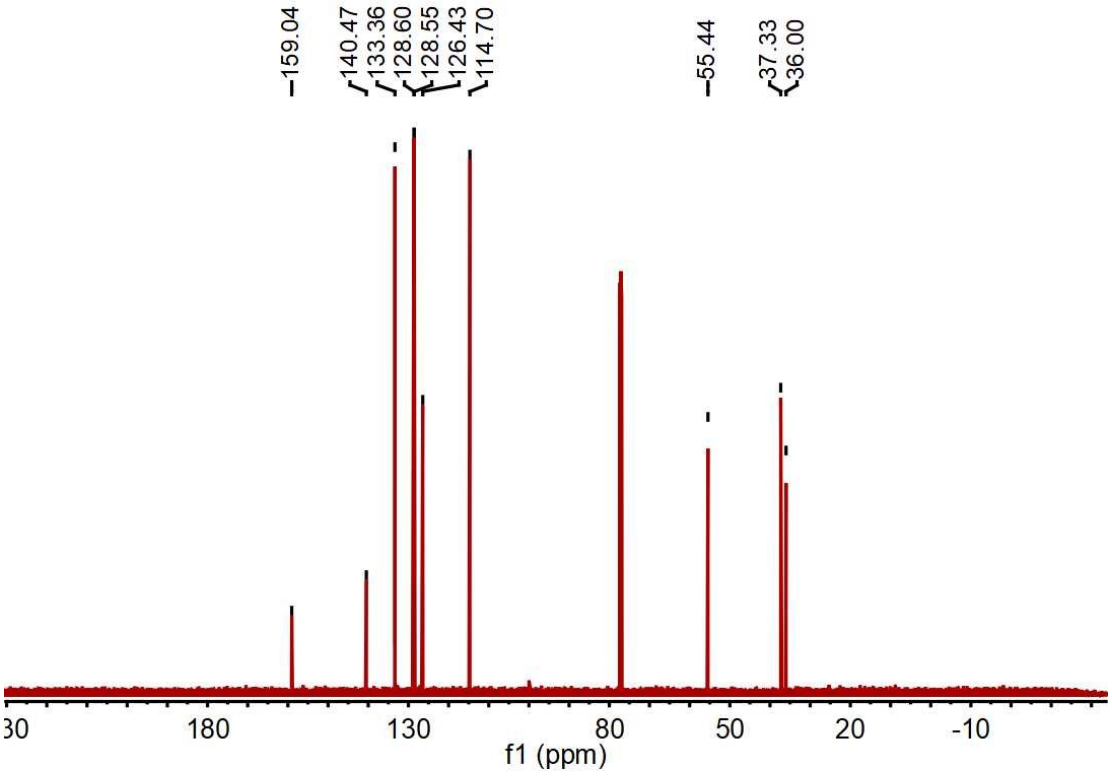
159.04
140.47
133.36
128.60
128.55
126.43
114.70
55.44
37.33
36.00
180
130
80
50
20
-10
f1 (ppm)

3.

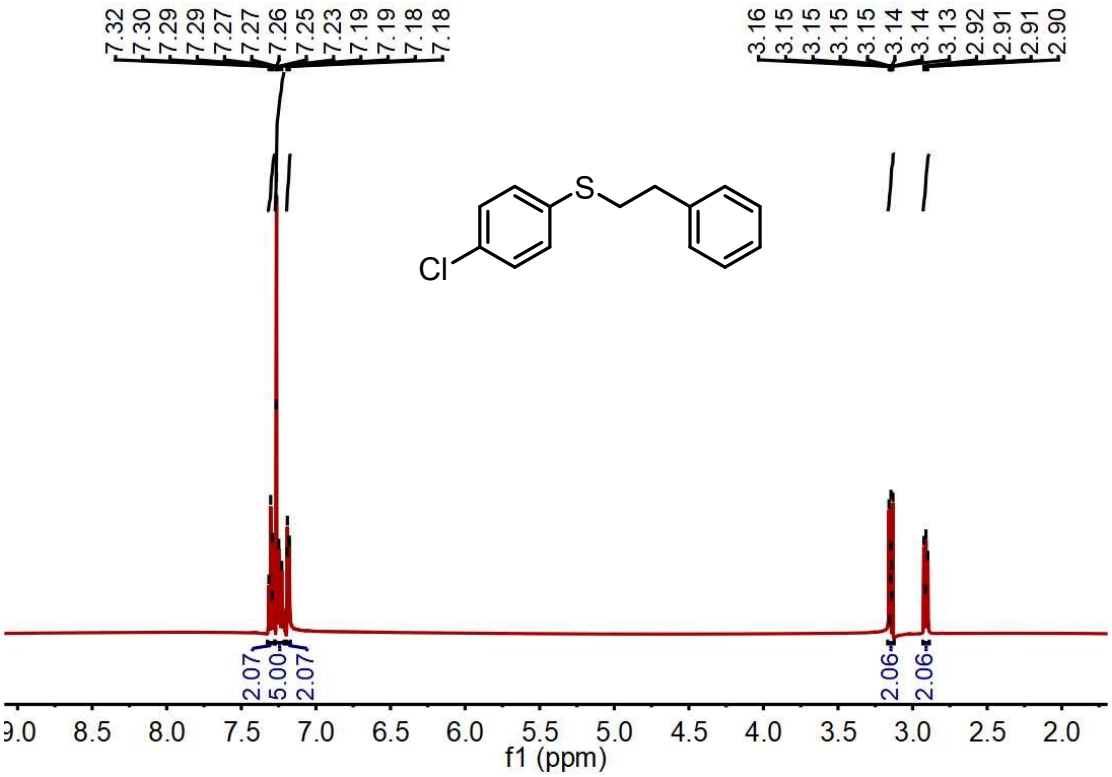
7.32
7.30
7.29
7.29
7.27
7.27
7.26
7.25
7.23
7.19
7.19
7.18
7.18
3.16
3.15
3.15
3.15
3.15
3.14
3.14
3.13
2.92
2.91
2.91
2.90
S
Cl
2.07
5.00
2.07
2.06
2.06
f1 (ppm)

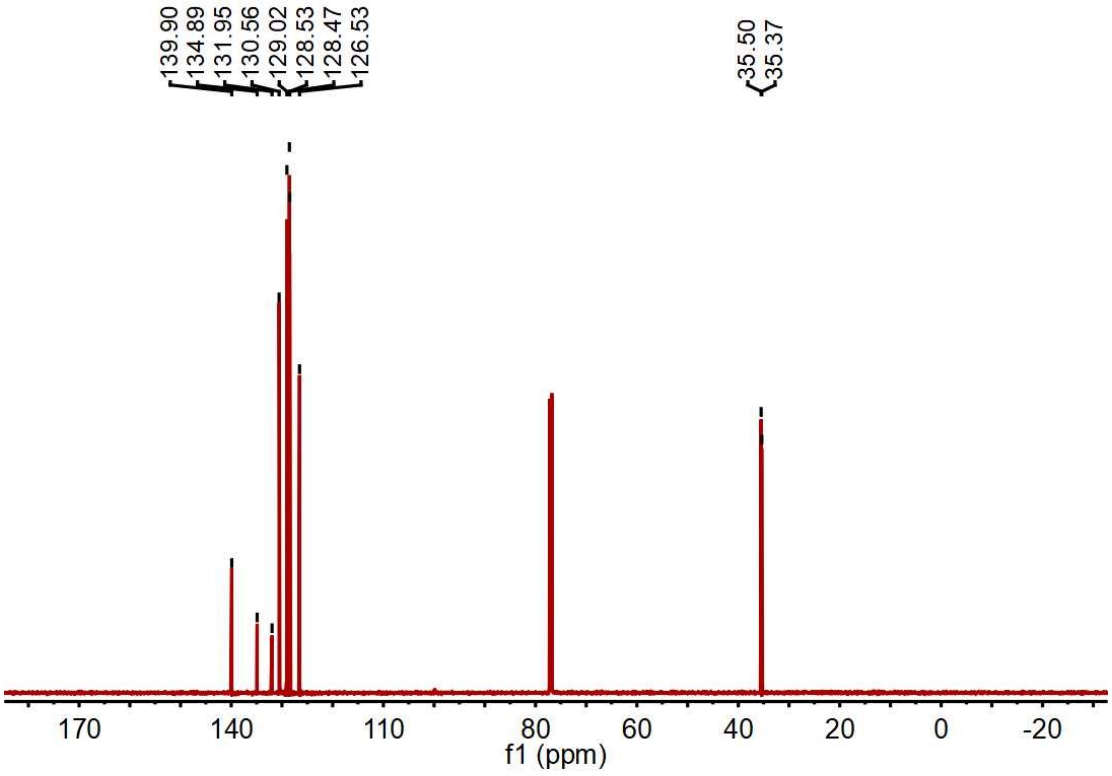
139.90
134.89
131.95
130.56
129.02
128.53
128.47
126.53
35.50
35.37
f1 (ppm)

4.

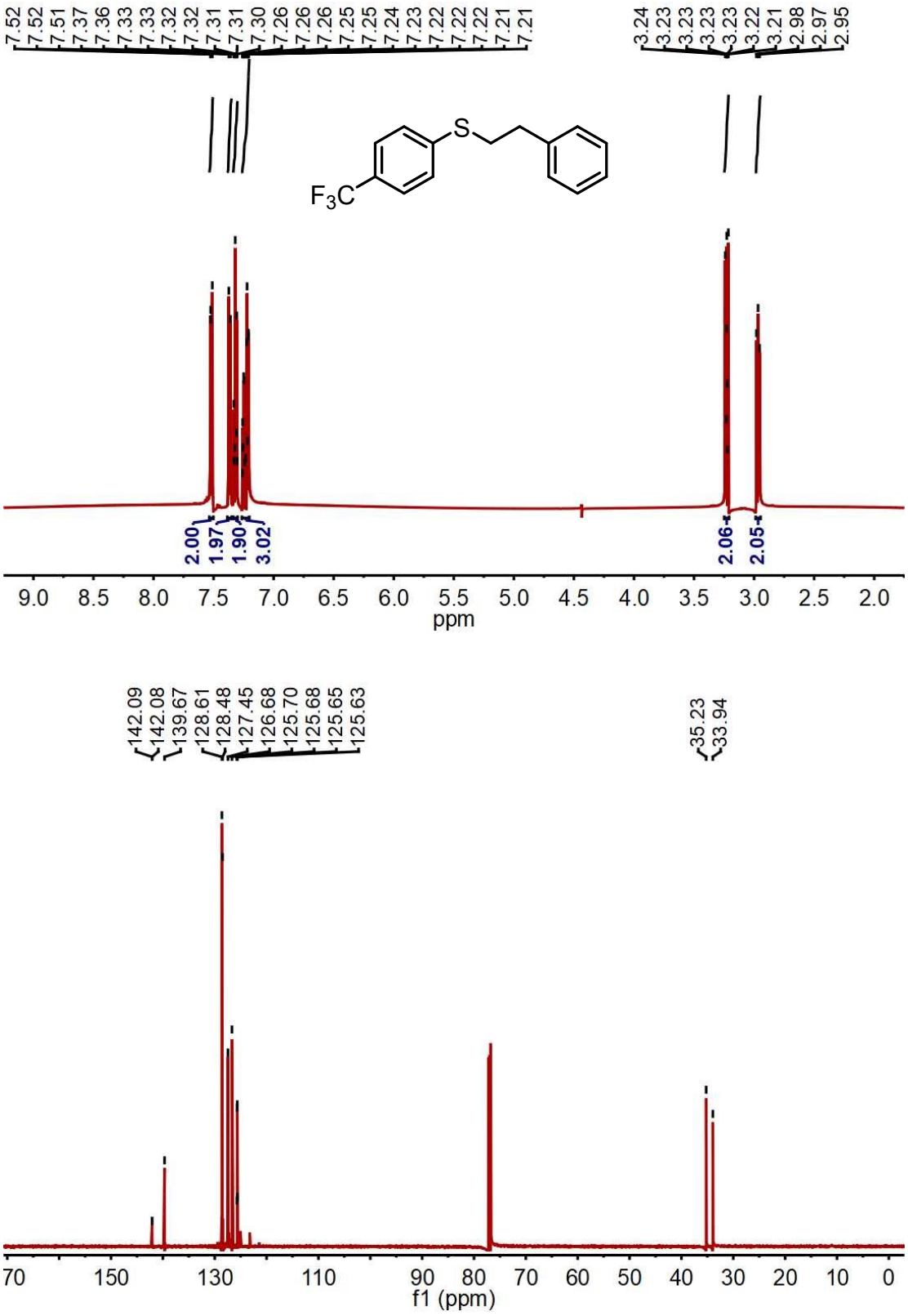

Figure S18. The NMR spectra of the reaction products.

Optimized Geometries

1. Optimized geometry of complex 5C (IN1': FeIIIPor-PhSH)

Fe	0.63524300	-0.00227300	-0.37446800
N	1.28636900	-1.95600800	-0.42851900
N	-0.95507100	-0.54949900	-1.55723000
N	0.28401700	1.96200000	-0.88896400
N	2.51398100	0.55579200	0.26301600
C	3.48057500	-1.67944600	0.66617900
C	-0.66846000	-3.00009900	-1.51127400
C	-1.36965000	-1.84137800	-1.84525900
C	-1.90905200	0.29204900	-2.10939000
C	1.29269400	-4.26512200	-0.57049900
C	2.46091100	-3.89259300	0.04256000
C	2.45578200	-2.45581500	0.12501700
C	0.56655900	-3.05802300	-0.86592200
C	-2.94609600	-0.48645600	-2.73282200
C	-2.61321100	-1.80634000	-2.56801200
C	2.28330600	3.00787000	0.11172200
C	2.97313200	1.84962700	0.47001400
C	1.04594300	3.06499100	-0.53100100
C	-1.85546100	1.68562500	-2.08755900
C	4.27388600	1.81359600	1.08358700
C	3.51823600	-0.28663500	0.72211100
C	4.61047500	0.49327600	1.23924400
C	-0.78235400	3.90035800	-1.56593500
C	0.38130700	4.27303500	-0.94380200
C	-0.83767500	2.46269600	-1.53487700
H	0.95347300	-5.27034000	-0.80928600
H	3.26172000	-4.53423800	0.40241000
H	-3.81457500	-0.07395300	-3.24082400
H	-3.15625200	-2.68193700	-2.91575200
H	4.86028400	2.68911900	1.35230000
H	5.52494600	0.08176700	1.65988800
H	-1.53442500	4.54289400	-2.01782700
H	0.76429400	5.27892100	-0.78835100
H	4.34527000	-2.21237900	1.06472700
H	2.77053700	3.95962900	0.32981500
H	-2.67636300	2.21846300	-2.57010100
H	-1.11685200	-3.95030500	-1.80581600
C	-4.07028300	-1.25096000	2.40278300

C	-2.67634600	-1.21639400	2.32771200
C	-2.03490400	0.00711200	2.08814000
C	-2.77065600	1.18901700	1.92637500
C	-4.16279300	1.13942600	2.02015300
C	-4.81415700	-0.07656400	2.25304300
H	-4.57356600	-2.19972500	2.59510100
H	-2.09432400	-2.12839000	2.47223600
H	-4.73998700	2.05906800	1.91113000
S	-0.24866200	-0.01977900	2.02519700
H	-0.03781500	1.30238100	2.24010900
H	-2.26714700	2.13834000	1.73645800
H	-5.90227000	-0.10687100	2.32494600

2. Optimized geometry of complex 6C (IN1: PhSH-FeIIIPor-O_2)

Fe	-0.67321400	0.05522300	0.46131200
N	0.96336200	0.74555400	1.34447800
N	-1.26149900	1.92401200	0.09904200
N	-2.25483600	-0.63679900	-0.56183600
N	-0.03372800	-1.81943500	0.74017400
C	2.05383000	-1.38070100	1.97069800
C	0.56188000	3.17348600	1.18410800
C	-0.63854400	3.09808300	0.49545100
C	-2.41586800	2.33129800	-0.56737400
C	2.54128000	2.15238600	2.30190400
C	2.96074100	0.87001600	2.52272100
C	1.98365100	0.00011400	1.93343700
C	1.30486000	2.07193200	1.57630800
C	-2.50844000	3.76334900	-0.57361900
C	-1.40868200	4.23894400	0.08587200
C	-1.87572900	-3.06364300	-0.33443200
C	-0.68229200	-2.98949100	0.36932100
C	-2.60642400	-1.96433800	-0.76266000
C	-3.35054000	1.49191300	-1.14756200
C	0.06049500	-4.13366000	0.81655900
C	1.10470100	-2.22807100	1.41435700
C	1.17017100	-3.66053000	1.46522100
C	-4.26117100	-0.76296100	-1.71161100
C	-3.84807100	-2.04791000	-1.47703400
C	-3.27388200	0.10514600	-1.13808800
H	3.01651000	3.08115500	2.60800200
H	3.85082400	0.53085300	3.04686700
H	-3.32062900	4.32632800	-1.02690200

H	-1.13400100	5.27213400	0.28398100
H	-0.24041900	-5.16627800	0.65725200
H	1.96345200	-4.22624200	1.94773300
H	-5.16106200	-0.42492000	-2.21946500
H	-4.34008600	-2.97684400	-1.75471100
H	2.90704900	-1.83326400	2.47625200
H	-2.27196000	-4.05443300	-0.55804400
H	-4.21045800	1.94956700	-1.63703600
H	0.94240600	4.16258500	1.43973500
C	4.25198900	1.17474100	-2.04222500
C	2.85776400	1.18461500	-1.98262900
C	2.16144700	-0.03388500	-1.94699400
C	2.85343100	-1.25430100	-1.97124300
C	4.24727600	-1.24780600	-2.04309000
C	4.94873200	-0.03775000	-2.07449500
H	4.79465000	2.12068900	-2.07779400
H	2.31426100	2.13131300	-1.98122500
H	4.78684900	-2.19570300	-2.07802800
S	0.38428900	0.04727900	-1.91127900
H	0.15324900	-1.26471000	-2.15652700
O	-1.65944400	-0.00562300	2.09574500
O	-2.35229700	-0.99216200	2.42462200
H	2.31136900	-2.20127600	-1.94491200
H	6.03813900	-0.04010000	-2.13217000

3. Optimized geometry of O_2-FeIIIPor-CH_3OH

Fe	-0.03481500	0.01903500	0.09238200
N	1.06558600	-1.62036200	0.01974000
N	1.63413200	1.13740700	0.11216600
N	-1.13641700	1.70288100	0.00082600
N	-1.69175900	-1.06312700	-0.03517700
C	-0.71617200	-3.32584800	-0.06773300
C	3.33222700	-0.64711800	0.17717300
C	2.94396000	0.68492500	0.18259600
C	1.72240400	2.52128600	0.15037600
C	2.85861500	-3.09078500	0.09903100
C	1.71844600	-3.84586700	0.02540000
C	0.61195800	-2.93550600	-0.01630700
C	2.45463900	-1.71557600	0.10059900
C	3.09619500	2.93184900	0.23583400
C	3.85385500	1.79177900	0.25791000
C	-3.39849000	0.72264300	-0.04550000

C	-3.00543100	-0.60518000	-0.06200900
C	-2.52275300	1.79796000	-0.01060700
C	0.65010000	3.40054300	0.12075700
C	-3.91737900	-1.71177500	-0.11535100
C	-1.78732600	-2.44715200	-0.07448000
C	-3.16291000	-2.85330600	-0.12352200
C	-1.78778300	3.92706900	0.06463000
C	-2.93001800	3.17257500	0.02186900
C	-0.68033800	3.01382000	0.06014000
H	3.88996700	-3.43020500	0.15660700
H	1.62629700	-4.92909500	0.00932000
H	3.43000100	3.96578500	0.27800100
H	4.93534500	1.70006400	0.32128100
H	-5.00020600	-1.61740100	-0.14119300
H	-3.50050900	-3.88619500	-0.15849400
H	-1.69477600	5.00970100	0.10320200
H	-3.96315500	3.51124300	0.01814400
H	-0.93227400	-4.39395400	-0.09488800
H	-4.46732200	0.93670200	-0.05915400
H	0.86715800	4.46807300	0.16315300
H	4.39789500	-0.86784000	0.24107000
C	1.05962300	-0.10674600	-3.00139100
H	1.40796600	-1.12325100	-2.79337700
H	0.72133800	-0.04238500	-4.04503600
H	1.87167500	0.61172500	-2.81854400
O	-0.06707500	0.13311400	-2.11821400
H	-0.43570000	1.01773400	-2.30302700
O	-0.08271800	0.03788800	1.98989900
O	-0.31393700	-0.99609400	2.64851900

4. Optimized geometry of PhSH-O_2

C	4.25198900	1.17474100	-2.04222500
C	2.85776400	1.18461500	-1.98262900
C	2.16144700	-0.03388500	-1.94699400
C	2.85343100	-1.25430100	-1.97124300
C	4.24727600	-1.24780600	-2.04309000
C	4.94873200	-0.03775000	-2.07449500
H	4.79465000	2.12068900	-2.07779400
H	2.31426100	2.13131300	-1.98122500
H	4.78684900	-2.19570300	-2.07802800
S	0.38428900	0.04727900	-1.91127900
H	0.15324900	-1.26471000	-2.15652700

O	-1.65944400	-0.00562300	2.09574500
O	-2.35229700	-0.99216200	2.42462200
H	2.31136900	-2.20127600	-1.94491200
H	6.03813900	-0.04010000	-2.13217000

5. Optimized geometry of the low spin FeIIIPor (*S = 1/2*)

Fe	-0.00004700	0.00007100	0.09478400
N	-1.69556600	1.02925100	-0.01385900
N	1.02936300	1.69550600	-0.01484200
N	1.69570300	-1.02930000	-0.01380000
N	-1.02945800	-1.69552400	-0.01469000
C	-3.32790700	-0.81359700	-0.03294900
C	-0.81353300	3.32757700	0.01560900
C	0.53393800	2.99199200	0.00018900
C	2.40832900	1.85407200	-0.02819000
C	-3.24267200	2.76889500	-0.00908800
C	-3.95265600	1.59949800	-0.02894300
C	-2.99214700	0.53378800	-0.02641800
C	-1.85414700	2.40815600	0.00193800
C	2.76876300	3.24273900	-0.03243300
C	1.59935500	3.95271400	-0.01258400
C	0.81352700	-3.32759700	0.01569000
C	-0.53392000	-2.99200800	0.00029700
C	1.85418100	-2.40814600	0.00197500
C	3.32790400	0.81363000	-0.03294700
C	-1.59931600	-3.95274000	-0.01265200
C	-2.40827900	-1.85412500	-0.02821200
C	-2.76876100	-3.24275700	-0.03250700
C	3.95269100	-1.59948900	-0.02898700
C	3.24266600	-2.76894800	-0.00914700
C	2.99212300	-0.53386600	-0.02645200
H	-3.61891700	3.78885200	-0.00379800
H	-5.03109400	1.46313300	-0.04274100
H	3.78859400	3.61907200	-0.04723100
H	1.46281900	5.03120900	-0.00832900
H	-1.46278500	-5.03123600	-0.00842600
H	-3.78858500	-3.61910100	-0.04742000
H	5.03112900	-1.46313400	-0.04276500
H	3.61892300	-3.78890000	-0.00386100
H	-4.38743200	-1.07266400	-0.04157400
H	1.07256700	-4.38708000	0.02928000
H	4.38743400	1.07267000	-0.04155800

H	-1.07256400	4.38706500	0.02924400

6. Optimized geometry of the high spin FeIIIPor (*S = 5/2*)

Fe	0.00001000	0.00000500	0.20165200
N	-1.91490800	0.68728000	-0.01101100
N	0.68729100	1.91490200	-0.01093900
N	1.91491400	-0.68729200	-0.01095900
N	-0.68730500	-1.91489900	-0.01102400
C	-3.11319700	-1.46869400	-0.02770600
C	-1.46869300	3.11317800	-0.02749100
C	-0.07305500	3.07559200	-0.02614800
C	2.01221300	2.32723300	-0.02626300
C	-3.76308000	2.07946200	-0.04869600
C	-4.22651500	0.78811200	-0.04874000
C	-3.07560200	-0.07305500	-0.02621700
C	-2.32723300	2.01220600	-0.02610600
C	2.07945700	3.76307500	-0.04897700
C	0.78810100	4.22650300	-0.04889900
C	1.46868700	-3.11317900	-0.02751000
C	0.07304700	-3.07558400	-0.02614400
C	2.32724200	-2.01221200	-0.02613100
C	3.11318800	1.46869200	-0.02763200
C	-0.78810400	-4.22650300	-0.04882000
C	-2.01222100	-2.32723600	-0.02630900
C	-2.07946200	-3.76308100	-0.04893000
C	4.22651500	-0.78810600	-0.04875500
C	3.76308500	-2.07946400	-0.04876000
C	3.07559900	0.07305100	-0.02616200
H	-4.34441500	2.99824200	-0.06365400
H	-5.25943000	0.44866900	-0.06375200
H	2.99822900	4.34441700	-0.06411600
H	0.44865700	5.25941700	-0.06396800
H	-0.44865800	-5.25941900	-0.06380000
H	-2.99823100	-4.34442900	-0.06402200
H	5.25943100	-0.44866700	-0.06377200
H	4.34442900	-2.99823600	-0.06379300
H	-4.10011900	-1.93442700	-0.04071600
H	1.93441000	-4.10010700	-0.04043100
H	4.10010900	1.93442700	-0.04063100
H	-1.93442900	4.10010000	-0.04041400

References

[1] M. J. Frisch, G. W. T., H. B. Schlegel, G. E. Scuseria, M. A. Robb, J. R. Cheeseman, G. Scalmani, V. Barone, B. Mennucci, G. A. Petersson, H. Nakatsuji, M. Caricato, X. Li, H. P. Hratchian, A. F. Izmaylov, J. Bloino, G. Zheng, J. L. Sonnenberg, M. Hada, M. Ehara, K. Toyota, R. Fukuda, J. Hasegawa, M. Ishida, T. Nakajima, Y. Honda, O. Kitao, H. Nakai, T. Vreven, J. A. Montgomery, Jr., J. E. Peralta, F. Ogliaro, M. Bearpark, J. J. Heyd, E. Brothers, K. N. Kudin, V. N. Staroverov, R. Kobayashi, J. Normand, K. Raghavachari, A. Rendell, J. C. Burant, S. S. Iyengar, J. Tomasi, M. Cossi, N. Rega, J. M. Millam, M. Klene, J. E. Knox, J. B. Cross, V. Bakken, C. Adamo, J. Jaramillo, R. Gomperts, R. E. Stratmann, O. Yazyev, A. J. Austin, R. Cammi, C. Pomelli, J. W. Ochterski, R. L. Martin, K. Morokuma, V. G. Zakrzewski, G. A. Voth, P. Salvador, J. J. Dannenberg, S. Dapprich, A. D. Daniels, Ö. Farkas, J. B. Foresman, J. V. Ortiz, J. Cioslowski and D. J. Fox, *Gaussian 09, Revision D.01*, Gaussian Inc., Wallingford, CT, 2009.

[2] T. Lu and F. Chen, *J. Comput. Chem.*, 2012, **33**, 580-592.

[3] J. Zhang and T. Lu, *Phys. Chem. Chem. Phys.*, 2021, **23**, 20323-20328.

[4] W. Humphrey, A. Dalke, K. Schulten, *J. Mol. Graph*, 1996, **14**, 33-38.